

Supporting Information

Dual dimensional nanostructures with highly durable non-wetting properties in dynamic and underwater conditions

Seunghyeon Baek,^a Wuseok Kim,^b Sangmin Jeon,^b Kijung Yong^{*a}

^aSurface chemistry Laboratory of Electronic Materials, Department of chemical engineering, Pohang University of Science and Technology (POSTECH), Pohang 37673, Korea

^bSmart Materials Sensors Laboratory, Department of chemical engineering, Pohang University of Science and Technology (POSTECH), Pohang 37673, Korea

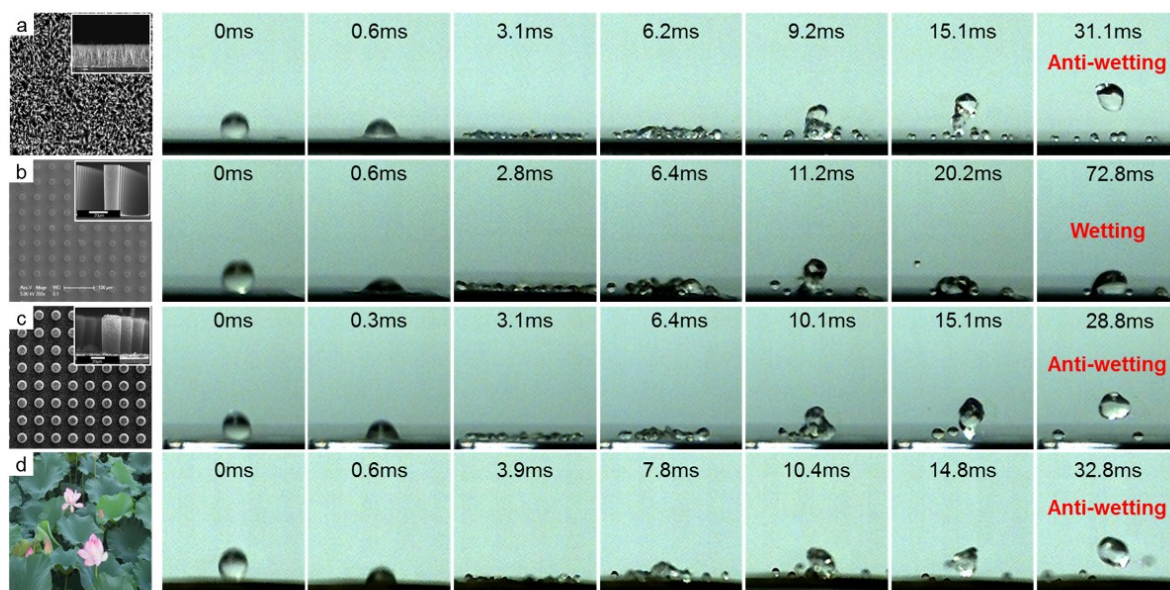


Fig. S1 Snapshots of the impact dynamics of water droplets on the various sample surfaces: (a) ZnO-NWs, (b) Si-MPs, (c) ZnO/Si HNs and (d) LL. The frame rate of the high-speed camera was 3600fps, and the We number was 98.8

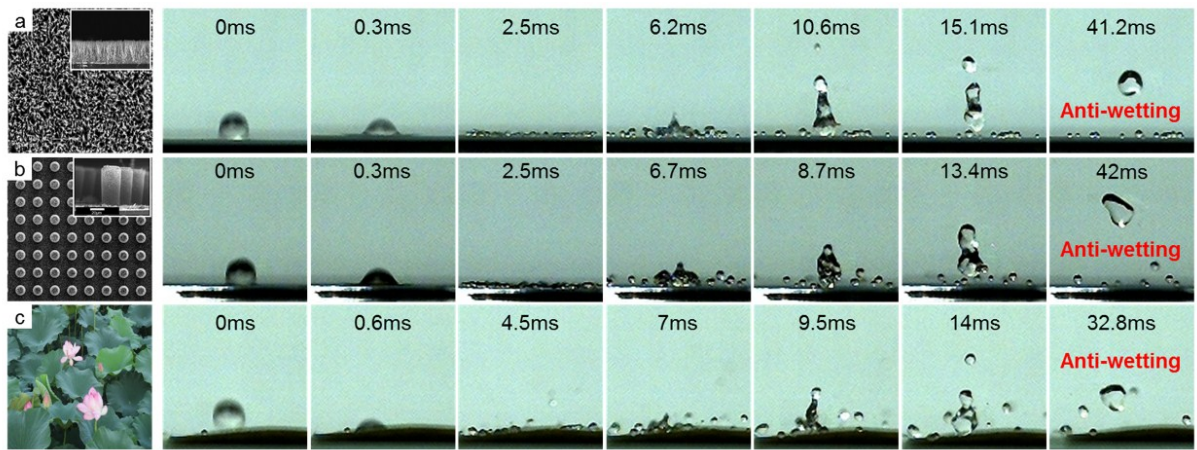


Fig. S2 Snapshots of the impact dynamics of water droplets on the various sample surfaces: (a) ZnO-NWs, (b) ZnO/Si HN and (c) LL. The frame rate of the high-speed camera was 3600 fps, and the We number was 180 ($h=60\text{cm}$)

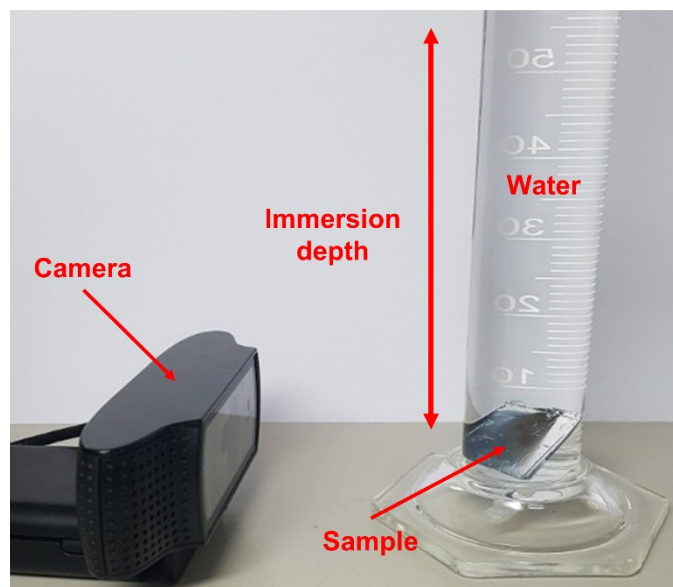


Fig. S3 Experimental set-up for underwater stability test. When the incident light illuminates the superhydrophobic surface with an incident angle $\sim 50^\circ$, total reflection occurs. The camera monitors the surface with time and then the relative intensity of bright pixel from mirror-like surface is plotted as a function of time for determining the decay time. The immersion depth is fixed at 20 cm in this experiment.

Spacing	Capillary pressure (Si-MPs)	Capillary pressure (ZnO-Si HNs)
30 μm	1.13 kPa	2.80 kPa
50 μm	0.54 kPa	1.31 kPa
100 μm	0.18 kPa	0.42 kPa

Table. S1 The capillary pressures of 30, 50 and 100 μm spacing Si-MPs and ZnO/Si HNs evaluated by our model.

Supporting Note. 1 Calculation of the capillary pressure

The capillary pressure which interrupts the intrusion of the water droplet expressed by Torkkeli in rough surface like (1);¹

$$P_C = -\gamma_{LA} \cos \theta \frac{L_C}{A_C} \quad (1)$$

where γ_{LA} is the surface energy of water (72 mN/m), θ is the contact angle of water, L_C is the perimeter and A_C is the cross-sectional area of the air pocket. To apply these pressures to our system, we modeled Si-MPs as shown in Fig. 5. In Si-MPs, the cross-sectional area of the air pocket is $A_c = P^2 - \pi r^2$, the perimeter is $L_C = 2\pi r$

and the fraction of the solid is $\phi = \frac{\pi r^2}{P^2}$, where P is the interspacing of microposts and r is the radius of the cross-section of the micropost. As a result, the capillary pressure is modified like (2);

$$P_C = \frac{-2\pi r \gamma_{LA} \cos \theta}{P^2 - \pi r^2} \quad (2)$$

Eq. (2) expresses the capillary pressure of Si-MPs in our system. To clarify the meaning of roughness, the fraction of solid ϕ is introduced like (3);

$$P_C = \frac{-2\pi r \gamma_{LA} \cos \theta}{P^2 - \pi r^2} = -2\gamma_{LA}(\cos \theta) \frac{\frac{\pi r}{P^2}}{1 - \frac{\pi r^2}{P^2}} = -2\gamma_{LA}(\cos \theta) \frac{\phi}{r(1 - \phi)} \quad (3)$$

Like Si-MPs, ZnO/Si HNs also could be obtained from Eq. (1). In this case, the perimeter and cross-sectional area of the air pocket are defined as; $A_c = P^2 - \pi(r + l)^2 + \alpha$, and $L_C = 2\pi(r + l)$. Thus, the capillary pressure of ZnO/Si HNs is transformed to Eq. (4);

$$P_C = \frac{-2\pi \gamma_{LA}(\cos \theta)(r + l)}{P^2 - \pi(r + l)^2 + \alpha} \quad (4)$$

Supporting Note. 2 Calculation of the α (additional air pocket)

As growth of the ZnO nanowires on the Si-MPs, the additional air pocket is generated from the ZnO nanowires. So, we should introduce new parameter α to calculate the additional air pocket. α can also be deduced like unit cell of Si-MPs. Thus, α is calculated like (1);

$$\alpha = \frac{P'^2 - r'^2}{P'^2} \times \pi r'^2 \quad (1)$$

where P' is the spacing of ZnO nanowires and r' is the radius of ZnO nanowires. The FE-SEM images are captured to specify the formula. The ZnO nanowires have spacing of about 600nm and radius of 75nm as shown in Fig. S4. Through the results, α is obtained in eq (2).

$$\alpha = \frac{(600 \times 10^{-9})^2 - (75 \times 10^{-9})^2}{(600 \times 10^{-9})^2} \times \pi(10 \times 10^{-6})^2 = 3.09 \times 10^{-10} \quad (2)$$

α elucidate the physical meaning of the contact between water droplet and top of ZnO/Si-MPs. The calculated

value of $\frac{P'^2 - r'^2}{P'^2}$ is 0.98 in above case. It implies that the top of micropost has 98% of air fraction. If the water droplet contacts the microposts, the water droplet rarely touches the solid part. Thus, the dual dimensional air pocket enables ZnO/Si HN to show anti-wetting property in impact dynamics testing and to have the high stability in underwater.

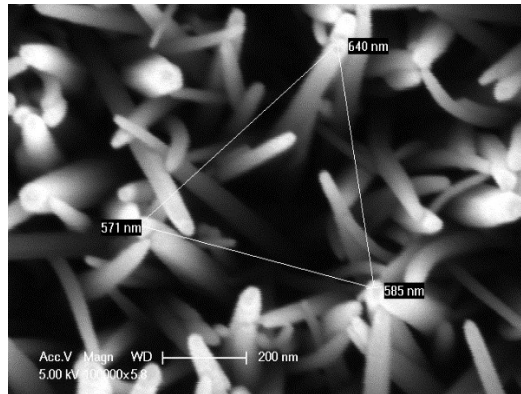


Fig. S4 Field emission SEM image of ZnO nanowires. The average spacing of the ZnO nanowire is about 600nm and radius is about 75nm.

Supporting Note. 3 Factors affecting the underwater stability

It is well known that superhydrophobic surfaces lose their property under the water because of the thermodynamic instability of air pocket. In the underwater condition, the air gases diffuse into the water continuously and thus non-wetting surface has limited life-time (or decay time) in the submerged underwater condition. Poetes *et al.*² deduced the correlation between underwater stability and immersion depth. They said that the superhydrophobic surface was preserved in a water for a moment. However, it lost their superhydrophobicity rapidly as increasing the hydrostatic pressure. The tendency of decline of stability is expressed in equation (1)

$$\ln \left(\frac{p'}{p_0} \right) = \frac{\bar{v}}{RT} [p(h) - p_0] \quad (1)$$

where p' is the fugacity of the air, p_0 is the atmospheric fugacity, \bar{v} is the partial molar volume, R is the gas constant, T is the temperature and p_0 is the atmospheric pressure. In here, hydrostatic pressure could be expressed like;

$$p(h) = p_0 + \rho gh \quad (2)$$

where p_0 is the atmospheric pressure, ρ is the density of the water, g is the gravitational acceleration, and h is the immersion depth. From the equation (1) and (2), the fugacity of the air increases exponentially as increasing the immersion depth. Thus, the decay time decreased rapidly at high immersion depth due to fast mass transport of gases into water. Fig. S5a shows the experimental result.³

Besides the hydrostatic pressure, the Laplace pressure also could affect the fugacity. The Laplace pressure is known as resistive pressure against penetration of the water droplet. The equation (3) shows the Laplace pressure

$$P_L = \frac{2\gamma \cos \theta_0}{d} \quad (3)$$

where, γ is the surface energy of water, θ_0 is the contact angle of water droplet on smooth surface, and d is the distance of roughness. Because the Laplace pressure could offset the hydrostatic pressure, the equation (1) should be transformed like (4);³

$$\ln \left(\frac{p'}{p_0} \right) = \frac{\bar{v}}{RT} \left[p(h) - \frac{2\gamma \cos \theta_0}{d} - p_0 \right] \quad (4)$$

The equation (4) shows the underwater stability could be also affected by the surface energy as seen in Fig. S5b.

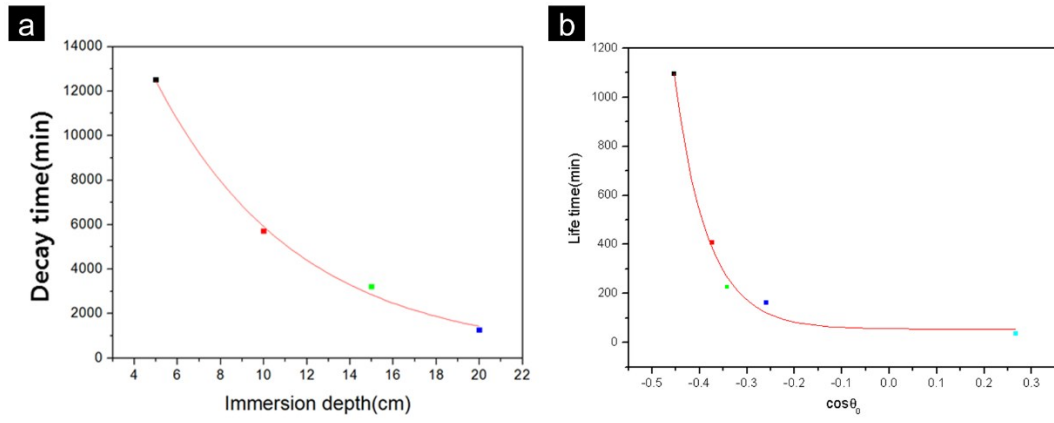


Fig. S5 Underwater stability test results as functions of (a) the immersion depth and (b) surface energy

References

- 1 A. Torkkeli, "Droplet microfluidics on a planar surface", VTT publications, 2003.
- 2 R. Poetes, K. Holtzmann, K. Franze and U. Steiner, *Phys. Rev. Lett.*, 2010, **105**, 1–4.
- 3 J. Lee and K. Yong, *J. Mater. Chem.*, 2012, **22**, 20250–20256.